Simple model for crystal shapes: Step-step interactions and facet edges

C. Jayaprakash, Craig Rottman, and W. F. Saam
Physics Department, The Ohio State University, Columbus, Ohio 43210
(Received 9 July 1984)

The terrace-step-kink model for equilibrium crystal shapes is considered. Noninteracting steps are known to correspond to a free-fermion model which leads to a continuous transition from facets to curved surfaces. We study both short- and long-ranged interactions between steps within mean-field theory. For nearest-neighbor step interactions, the model can be solved exactly, and details are given. The possibility of a slope discontinuity between facets and curved surfaces is explored within the interacting terrace-step-kink model (which ignores voids and overhangs); this possibility is realized only for sufficiently long-ranged attractive interactions. As physical examples of such interactions we consider both elastic and dipolar interactions between steps. These have the same range, and may be comparable in magnitude. It is argued that elastic interactions (which are repulsive) do not change the free-fermion predictions for the exponent governing the facet-curved surface edge while dipolar interactions, if attractive, can lead to slope discontinuities and associated tricritical phenomena.

I. INTRODUCTION

The topic of equilibrium crystal shapes (ECS) is currently of considerable interest.[1-9] The physics of facets and curved surfaces which constitute the ECS and their thermal evolution can be described in terms of the venerable terrace-step-kink (TSK) model,[10,11] in which an interface of orientation $\hat{n}$ possesses steps which separate flat terraces of orientation $\hat{n}_0$. The density of steps determines the slope of $\hat{n}$ with respect to $\hat{n}_0$. At finite temperatures, the steps meander due to kinks excited within them. Steps are assumed to neither cross nor overlap due to the large energy cost of multiple-height steps and overhangs. Voids beneath the terraces are also tacitly neglected. Furthermore, steps are not allowed to terminate (due to high-energy costs of dislocations) and hence run across the entire surface. The model is thus best suited to describe low-temperature and low-step-density situations. The interfacial free energy $\gamma(\hat{n})$ was calculated by Gruber and Mullins[11] (in a somewhat simplified version of the TSK model) for the case of noninteracting steps. In particular, they computed the entropic contribution due to both the wandering of steps and the restriction of noncrossing. Essentially identical considerations have arisen recently in the context of commensurate-incommensurate (*C-I*) phase transitions in two-dimensional adsorbates.[12-15] The correspondence arises from identifying steps between terraces with domain walls between commensurate regions. Thus facets correspond to commensurate phases, and curved (rough) surfaces to incommensurate phases. In the *C-I* problem the statistical mechanics of noncrossing domain walls has been studied by exploiting the mapping to a one-dimensional spinless free-fermion model.[13,15] We follow this procedure to study an *interacting* TSK model, focusing on the effect of long- and short-ranged interactions on the singular lines between distinct facets and those between facets and curved surfaces. This approach provides a simple and appealing discussion of ECS profiles.

To set the stage we review earlier work briefly. Consider two facets and a curved portion of a crystal surface connecting them. The curved portion can join a facet continuously [see Fig. 1(a)] or with a slope discontinuity [Fig. 1(b)]. These correspond to second- and first-order phase transitions, respectively.[1,4-9] The continuous transition can be characterized by an exponent θ defined by $z(x) \sim -x^{\theta}$ in Fig. 1(a). This geometry is a function of temperature T and can be displayed as a phase diagram in the T-x plane. Let the two facets be, for example, the (100) and (110) facets of a simple cubic crystal. A possible thermal evolution which leads to Fig. 1(a) is shown in Fig. 1(c). For $0 \leq T < T_c$, the facets join with a sharp

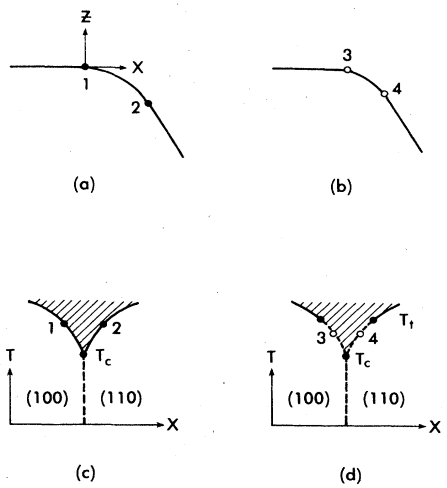

FIG. 1. Sketches of crystal-shape profiles [(a) and (b)] and associated phase diagrams [(c) and (d)]. In (c) and (d) solid lines indicate second-order (Pokrovsky-Talapov) transitions while dotted lines mark first-order transitions. Shaded regions indicate rough (curved) surfaces. See Sec. I for further details.

edge. For $T_c \leq T$ there is a curved portion between the facts which joins them continuously at boundaries shown by full lines. Such a picture has been found in an exact solid-on-solid (SOS) model calculation.[9] Figure 1(d) shows a situation which can lead to Fig. 1(b). Here the curved portion joins the facets discontinuously for $T_c < T < T_t$ (shown with a dashed line). At the tricritical temperature T_t the first-order line becomes second order. Figure 1(b) corresponds to a slice at $T_c < T < T_t$. This behavior has been found in a mean-field theory of an Ising lattice gas. Theory[1-4,9] also predicts $\theta = \frac{3}{2}$ for the continuous case, characterizing a transition known as the Pokrovsky-Talapov[12] (PT) or Gruber-Mullins[11] transition. Experiments show both first-order edges (in small gold crystals)[8] and second-order edges with $\theta = 1.60 \pm 0.15$,[6] consistent with theory (in small Pb crystals).

The TSK model will produce a phase diagram like that of Fig. 1(c) for the case of short-ranged attractive interactions. In this case it is incapable of dealing with the vanishing (roughening) of the facets as T is increased. However, for the case of short-ranged repulsive interactions, the edge between the (100) and (110) facets is replaced by the (120) facet, which does roughen. Associated with roughening is a universal jump in crystal surface curvature obtained in other work[3,4,9] and recently observed in the elegant work on ^{4}He crystals by Gallet *et al.*[7]

The TSK model also provides a framework for the study of the effects of long-ranged interactions such as those which arise as a consequence of elasticity. Elastic interactions, which are repulsive, will be shown to be important at low temperatures. Dipolar interactions play a similar role if they are repulsive. It will be argued that attractive long-ranged dipolar interactions can give rise to tricritical behavior at facet edges, such as that shown in Fig. 1(d).

II. FERMION PICTURE

In order to render the TSK model tractable, we now proceed to map it onto a $T=0$ fermion problem. Let the steps in the TSK model run in the y direction. Periodic boundary conditions in this direction are imposed so that the slope of the crystal face is always in the x direction. One can describe a configuration of the model by specifying the x coordinates of each of the n steps at each of the y coordinates. This point of view leads naturally to a transfer-matrix description of the propagation of the steps from one row (y coordinate) to the next. Let $\hat{T}$ denote the $(n \times n)$ transfer matrix. For mathematical convenience we take the continuum limit in the y direction (lattice spacing $a_y \to 0$). This is not expected to change the physics qualitatively. In the limit $a_y \to 0$ we may write (see the Appendix)

$$\hat{T} = e^{-a_y \hat{H}} , \tag{1}$$

where $\hat{H}$ is a quantum Hamiltonian which describes fermion propagation along the Euclidean time (y) direction. As is well known, the free energy per unit length in the y direction (multiplied by $-1/k_B T a_y$) is given by the largest eigenvalue of $\hat{T}$. Thus the free energy per unit length in the y direction is given by the ground-state energy of $\hat{H}$.

The connection to the crystal-shape problem goes as follows. If $f(s)$ is the free energy per unit area of the TSK model for given (positive) slope s, then the crystal profile $z(x)$ is determined by[5]

$$\lambda z(x) = \tilde{f}(\eta)\,|_{\eta=-\lambda x} , \tag{2}$$

where $\tilde{f}(\eta) = \min_s [f(s) - \eta s]$ is the Legendre transform of $f(s)$ to the conjugate field variable η, and λ (equal to one-half the pressure difference between the crystal and the fluid surrounding it) is a parameter fixing the overall size of the crystal. We let $s=0$ correspond to no steps on the crystalline surface and $s=1$ to a step running along every column of our lattice. Thus s is the step density per site in the y direction.

In constructing $\hat{T}$ we make use of the following restrictions: (i) step number is conserved from row to row and (ii) steps do not cross. The matrix elements of $\hat{T}$ are then determined by a kink energy Γ, an energy η_0 for a unit length of a straight step, and an interaction energy U_{ij} between unit lengths of parallel straight pieces of steps labeled i and j. To render interactions between different rows (steps interacting at different values of y) tractable we treat them in an average way: We compute U_{ij} as the interaction between a unit length of step at i and an infinite straight step at j. We expect this approximation to preserve the qualitative physics of interest here.

The fermion representation of $H = a_y \hat{H}$ is (see the Appendix)

$$H = \eta_0 \sum_{i=1}^{N} a_i^\dagger a_i - \frac{t}{2} \sum_{i=1}^{N} (a_i^\dagger a_{i+1} + a_{i+1}^\dagger a_i) + \sum_{\substack{i<j \\ i,j=1}}^{N} U_{ij} a_i^\dagger a_i a_j^\dagger a_j + \text{const} , \tag{3}$$

where $a_i^\dagger$ is a fermion operator which creates a step at site i. The hopping matrix element t is given by $t = \beta^{-1} \exp(-\beta\Gamma)$, where $\beta = 1/k_B T$. The Pauli principle condition $(a_i^\dagger)^2 = 0$ guarantees that steps do not overlap. Note that the density of fermions $(1/N)\sum_i a_i^\dagger a_i$ is equal to s, the slope of the interface. The free energy $f(s)$ is computed from the ground-state energy $E_0(s)$ of H via

$$f(s) = \frac{1}{NA} E_0(s) + f_0 , \tag{4}$$

where $A = a_x a_y$ is a unit-cell area of the flat ($s=0$) crystal surface, and $f_0 = f(0)$ is a constant.

III. EFFECTS OF STEP-STEP INTERACTIONS

In this section we explore the effects of step-step interactions on the PT behavior that arises in the noninteracting TSK model. The latter corresponds to $U_{ij}=0$ in Eq. (3), in which case the ground state is readily analyzed, and which produces, for small s,

$$f(s) = f_0 + (\eta_0 s + b s^3 + \cdots)/A , \tag{5}$$

in which f_0 is a constant and $b=t\pi^2/6$. This is the same form as found by Gruber and Mullins.[11] The bs^3 term is an entropy piece arising from the no-overlap condition, and there is no s^2 term. The s and s^3 terms in Eq. (5) lead directly, via Eq. (2), to the PT transition at a facet edge.

We will now include U_{ij} in the continuum limit of the fermion model and investigate how it alters Eq. (5). This limit will restrict us to small s, i.e., near the $s=0$ facet, where Eq. (5) is exact. Global effects involving other facets are ignored. We invoke the Hartree-Fock version of perturbation theory to deal with the interactions. In this case, the correction f_U to Eq. (5) is

$$f_U=\frac{1}{Aa}\int_a^\infty dx\, U(x)sG(x)\ , \tag{6}$$

in which a is a short-distance cutoff taken equal to the step height, and $G(x)$ is the free-fermion pair correlation function given by[16]

$$G(x)=s\left[1-\frac{\sin^2(\pi sx/a)}{(\pi sx/a)^2}\right]\ . \tag{7}$$

Here s/a is the fermion wave vector. Combining Eqs. (6) and (7) produces

$$f_U=\frac{s^2}{A}\int_1^\infty du\, U(au)\left[1-\frac{\sin^2(\pi su)}{(\pi su)^2}\right]\ . \tag{8}$$

If $U(x)$ has a range much smaller than the distance between steps a/s, we may expand the term in large parentheses in Eq. (8) to find

$$f_U=\frac{\pi^2 s^4}{3A}\int_1^\infty du\, u^2U(au)\ . \tag{9}$$

Short-ranged interactions thus contribute to Eq. (5) in order s^4. The Pokrovsky-Talapov result is unaltered. Note that a simple Hartree approximation ignoring the step-step correlations of Eq. (7) would have given an s^2 term in place of Eq. (9).

If the potential $U(x)$ is sufficiently long ranged, i.e., $U(x)=g/x^\lambda$ for $\lambda\le 2$, the above argument fails, as more care is required in the evaluation of the integral in Eq. (8). We treat specifically the case $\lambda=2$, which is important by virtue of the fact that both elastic[17] and dipolar interactions between steps have the form ga^2/x^2. For elastic interactions $g>0$ since all steps have the same sign. Dipolar interactions can in principle have g of either sign (see Sec. V). Then, to lowest order in s, Eq. (8) becomes

$$f_U=\frac{\pi s^3 g}{A}\int_0^\infty dy\frac{1}{y^2}\left[1-\frac{\sin^2 y}{y^2}\right]=\frac{\pi^2 g}{3A}s^3\ . \tag{10}$$

Combining Eqs. (5) and (10) yields

$$f(s)=f_0+\left[\eta_0 s+\left[b+\frac{\pi^2 g}{3}\right]s^3+\cdots\right]\Big/A\ . \tag{11}$$

Thus, within the context of perturbation theory, if $b+\pi^2 g/3>0$, interactions varying as ga^2/x^2 will not affect the PT exponent $\theta=\frac{3}{2}$, which follows directly from the algebraic form of $f(s)$ in either Eq. (5) or (11).

As noted in Sec. I, the Rottman-Wortis mean-field results produced a tricritical point separating first- and second-order transitions at facet edges. This occurs here when $b+\pi^2 g/3=0$. Since $b=\pi^2 e^{-\beta\Gamma}/6\beta$, we see that the coefficient of s^3 will change sign at a temperature T_t, solving

$$|g|=k_B T_t e^{-\Gamma/k_B T_t}/2\ . \tag{12}$$

Simple analysis of $\tilde{f}(\eta)=f(s)-\eta s$ shows that, indeed, T_t is a tricritical point. One might well worry whether or not this argument is too dependent on the simple perturbation theory used. Fortunately, Sutherland[18] has solved exactly the continuum fermion problem with an interaction, $U(x)=ga^2/x^2$. He finds a coefficient of the s^3 term proportional to $[1+(1+4g/t)^{1/2}]^2$. His result reduces to our Eq. (11) for $g\ll 1$. Furthermore, the solution holds only for $g/t\ge -\frac{1}{4}$, making low T inaccessible in the crystal-shape problem. This is because for $g/t<-\frac{1}{4}$ the interaction overcomes the Pauli principle which, in the two-fermion problem, leads to bound states with arbitrarily large binding energy. Since a transition to a bound state as a function of chemical potential in the fermion problem is a first-order phase transition, one is led to suspect that cutting off the $1/x^2$ potential at small x would lead to well-behaved bound states and tricritical points separating the extended and bound-state regimes.

IV. NEAREST-NEIGHBOR INTERACTIONS

In this section we explore the consequences of nearest-neighbor interactions between steps. The Hamiltonian of Eq. (3) becomes, adding in the field η coupling to the slope,

$$H=(-\eta+\eta_0)\sum_i a_i^\dagger a_i-\frac{t}{2}\sum_i(a_i^\dagger a_{i+1}+a_{i+1}^\dagger a_i)$$
$$+U\sum_i a_i^\dagger a_i a_{i+1}^\dagger a_{i+1}+\text{const}\ . \tag{13}$$

Using the standard Jordan-Wigner transformation,[19] we rewrite this model as the quantum XXZ chain:

$$H\equiv H_{XXZ}=\tfrac{1}{2}(U+\eta_0-\eta)\sum_i\sigma_i^z$$
$$-\frac{t}{2}\sum_i(\sigma_i^x\sigma_{i+1}^x+\sigma_i^y\sigma_{i+1}^y)$$
$$+\frac{U}{4}\sum_i\sigma_i^z\sigma_{i+1}^z+\frac{N}{2}\left[\eta_0-\eta+\frac{U}{2}\right]\ , \tag{14}$$

where the σ_i^α's are Pauli spin operators. This model has been solved exactly by Yang and Yang,[20] and their results can be directly transcribed into the language of equilibrium crystal shapes. We consider two cases.

$U<0$. This corresponds to step attraction, and H_{XXZ} describes a ferromagnetic spin chain. The magnetization variable $y=(1/N)\sum_i\langle\sigma_z^i\rangle$ corresponds to $2s-1$, where s is the fermion number density (crystal-surface slope in the original problem). The anisotropy parameter Δ and the magnetic field H of Yang and Yang[20] are given by $\Delta=-U/2t$ and $H=(1/2t)[\eta-\eta_0-U]$.

A schematic phase diagram is displayed in Fig. 2(a). The boundary between the facets ($s=0$ and $s=1$) is first order and persists to a temperature T_c solving $U/2t=-1$. Within this model the two facets do not roughen. The transition between the curved parts and the facets belongs to the Pokrovsky-Talapov universality class. This is seen from the expansion for the free energy around $s=1$ ($y=1$) which yields

$$f=f_0+\frac{1}{2t}(\eta-\eta_0-2U-2t)(1-s)+\frac{\pi^2}{3}(1-s)^3+O((1-s)^4)\ . \tag{15}$$

A similar expansion exists around $s=0$.[20] There is no temperature range where the transition from faceted to curved surfaces is discontinuous in this model, in agreement with the analysis of Sec. III.

It is of interest to ask what types of phase diagrams result from standard approximations for the fermion model of Eq. (13). Via a straightforward analysis we find that the self-consistent Hartree-Fock approximation[21] produces Fig. 2(a) with associated PT exponents but with a spurious extension of the first-order line above the vertex at T_c.

$U>0$. This corresponds to step repulsion and H_{XXZ} describes an antiferromagnetic chain. For $t=0$, the ground state of the Hamiltonian varies from $s=0$ for $\eta<\eta_0$ to $s=\frac{1}{2}$ for η in the interval $[\eta_0, \eta_0+2U]$ and to $s=1$ for $\eta>\eta_0+2U$. These states correspond to having three facets at zero temperature. We note in passing that introducing further-neighbor repulsive interactions introduces new facets[22] (corresponding to fermion density waves with different periodicities) at $T=0$. Any repulsive interaction not cut off at a finite distance produces infinitely many facets between $s=0$ and $s=1$. The phase diagram, obtained using the analysis of Yang and Yang[20] for $\Delta<0$, is shown in Fig. 2(b). We comment on some of the important features which are the same as for SOS models and which have been discussed in detail elsewhere.[3,4,9] The free-energy expansion for the region near the central facet edge yields, for $(U/2t)<1$,

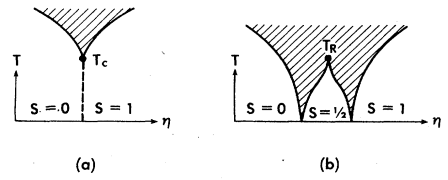

FIG. 2. Phase diagrams for the nearest-neighbor interacting TSK model in the cases of (a) attractive interactions and (b) repulsive interactions. Dotted lines are first-order transitions. Shaded regions indicate rough (curved) surfaces. In (b), T_R is the roughening temperature for the $s=\frac{1}{2}$ facet, while in (a), T_c is the (first-order) transition temperature at which the sharp edge between the $s=0$ and $s=1$ facets vanishes.

$$f=f_0+a\,|s-\tfrac{1}{2}|+b\,|s-\tfrac{1}{2}|^3+\cdots\ , \tag{16}$$

where a and b are positive constants which we do not display here [see Ref. 20(b), Eqs. (48)—(49)]. In addition, the facet with $s=\frac{1}{2}$ roughens (vanishes) at a temperature T_R defined by $U/2t=1$. As $T\to T_R^-$, $a\sim\xi_R^{-1}$, $b\sim\xi_R$, and the correlation length ξ_R diverges as $\exp[-c/(T_R-T)^{1/2}]$. This temperature dependence is expected to be universal; the constant c is not. For $T>T_R$, Eq. (16) is replaced by

$$f(s)=f_0+c(T)(s-\tfrac{1}{2})^2+\cdots\ , \tag{17}$$

where $c(T)$ is a temperature-dependent parameter. A self-consistent Hartree-Fock analysis for this case is not of great interest, since it fails to give roughening.[21]

V. DISCUSSION

Within the TSK model we have examined the effects of step-step interactions on crystal shapes. We have found that short-ranged interactions do not alter the Pokrovsky-Talapov transition at facet edges. We now amplify on this result by making a few comments regarding the occurrence of first-order transitions (between facets and curved surfaces) and tricritical points in global crystal shapes. In our problem curved surfaces arising from steps of orientation $\hat{m}$ (inaccessible to a description by a TSK model defined around orientation $\hat{n}$) might have lower free energy (and thus be part of the ECS) than the facet $\hat{n}$ or interfaces with orientation near $\hat{n}$. This will in general lead to a discontinuity in the slope. (This situation could possibly explain observations on gold crystals.[8]) If the step energy is too large, such a first-order transition is likely since the crystal prefers to change abruptly from facet to curved, rather than introduce costly steps. This suggests that impurities which tend to reduce step energies might in fact help in obtaining continuous facet-curved transitions. However, such a global mechanism is unlikely to lead to a tricritical point, though it could produce critical end points. Our analysis (Secs. III and IV) is limited in that it addresses the question of how changes in the *local* form of the interfacial free energy around $\hat{n}$ can lead to first-order transitions and tricritical points. We have argued that when voids and overhangs are neglected, short-range step-step interactions do not provide the mechanism for a first-order transition. Global mechanisms are *not* ruled out.

It is interesting to note that first-order transitions between a facet and a curved surface and between curved surfaces (due to a global mechanism) occur in the zero-temperature shape of a grain inclusion rotated with respect to the solid matrix of the same material.[23]

Long-ranged interactions varying as ga^2/x^2 do contribute to the s^3 term in $f(s)$ and the transition at facet edges is no longer governed by purely entropic effects. For $g<0$ a tricritical point probably appears, as noted in Sec. III. The case of $g>0$ is also of considerable physical interest. Both cases warrant more detailed discussion.

Elastic interactions between steps of the same sign have the form $U(x)=ga^2/x^2$, where, in order of magnitude[17]

(for an isotropic crystal)

$$g \sim \frac{\sigma^2 a}{E} , \tag{18}$$

where E is Young's modulus, σ is the surface tension, and a is an interatomic distance. The coefficient of the s^3 term in Eq. (11) then becomes

$$\left[b + \frac{\pi^2 g}{3} \right] = \frac{\pi^2}{6} \left[\frac{e^{-\beta\Gamma}}{\beta} + c \frac{\sigma^2 a}{E} \right] , \tag{19}$$

where c is a constant. It is clear from Eq. (19) that at sufficiently low T, elastic effects (as opposed to entropic effects) will dominate the transition at facet edges. Near enough to a roughening transition, however, b does not behave as shown in Eq. (19), but rather $b \sim \xi_R$.[9] Since $\xi_R \to \infty$ as $T \to T_R^-$, we expect that entropic effects become dominant near T_R.

For metals electrostatic interactions provide an additional source of long-ranged step interactions. There is both experimental[24] and theoretical[25] evidence that electronic charge-density distortions in pure metals give rise to line dipoles at steps. Furthermore, impurities clustering along steps will likely acquire dipole moments in the same way as do impurities on flat surfaces.[26] Let the dipole moment for a unit-cell length along the step be $\vec{p} = \vec{p}_{||} + \vec{p}_{\perp}$, where $\vec{p}_{||}$ is parallel to the surface containing the step and normal to the step direction, and where $\vec{p}_{\perp}$ is normal to both the step and the surface. Straightforward calculation produces an interaction $\sim a^2/x^2$, and use of Eq. (10) produces a contribution to f given by[27]

$$f_D = \frac{2\pi^3}{3} \frac{p_{\perp}^2 - p_{||}^2}{a^3} \frac{s^3}{A} . \tag{20}$$

This estimate neglects corrections of order unity[28] due to screening effects in the metal and any oscillatory effects of the Friedel type. Note that f_D can have either sign, depending on the direction of $\vec{p}$. If $p_{\perp} > p_{||}$, dipolar effects will add to the elastic effects in Eq. (19). Using the experimental result $|\vec{p}| \sim 0.1$–1.0 Debye for bare steps,[24] we find that the dipolar effect may well be comparable to elastic effects in metals. There will be an additional contribution to this effect from the dipole moment of impurities[26] which tend to accumulate at steps. If $p_{\perp} < p_{||}$, and f_D dominates elastic effects at low T, a tricritical point can occur at higher T when the entropic repulsion becomes sufficiently important, as in Eq. (12).

Finally, we note that the first-order edge appearing below T_c in Fig. 2(a) will be somewhat rounded in a real crystal as a consequence of elastic effects.[29]

While this work was being completed, we received a copy of unpublished work from H. J. Schulz (Institut Laue-Langevin, Grenoble) in which transfer-matrix methods were used to treat a solid-on-solid model for equilibrium crystal shapes. Phase diagrams similar to those in Fig. 2 were obtained.

ACKNOWLEDGMENTS

We wish to thank Professor Michael Wortis, Professor David Edwards, and Professor David Stroud, and Dr. Norton Lang and Ms. Yu He for useful conversations. One of us (C.J.) wishes to thank the Alfred P. Sloan Foundation and the National Science Foundation (Grant No. NSF-DMR-83-1577) for support. He is also grateful to the IBM Thomas J. Watson Research Center and the A.T.&T. Bell Laboratories for their hospitality. Another of us (C.R.) wishes to acknowledge the Ohio State University for financial support.

APPENDIX

For the benefit of the uninitiated reader, we provide a brief description of the fermion correspondence. We use techniques, outlined in Refs. 13 and 15, but we include effects of interactions. Consider a square lattice with M rows and N columns. Steps between terraces are specified by bonds on this lattice. A configuration is specified by a state vector $|x_1, \ldots, x_n\rangle_k$, where x_j denotes the position of the jth step in the kth row. The transfer matrix describes the propagation of the steps from row to row. The nonvanishing matrix elements are as follows: One is restricted to the subspace of fixed number of steps (steps do not end at any row). The position of a step can only change by $0, \pm 1$ units between rows. If, in going from row k to row $k+1$, the ordinates of p of the steps are unchanged while the other $(n-p)$ change by ± 1, then the matrix element has a contribution $e^{-\beta\eta_0 p - \beta\Gamma(n-p)}$ where Γ is a kink creation energy and η_0 is the step energy. The matrix element vanishes if $x_i = x_j$ for $i \neq j$ (walls do not cross). If, in addition, there is a step-step interaction energy, one obtains a multiplicative contribution $\exp(-\beta \sum_{i<j} U(x_i - x_j))$. A convenient operator representation is obtained by associating a step creation operator $a_j^{\dagger}$ for a step at x_j in row k: $a_j^{\dagger} a_j$ denotes a straight step while $a_{j+1}^{\dagger} a_j$ and $a_j^{\dagger} a_{j+1}$ denote a kink to the right and to the left, respectively. The a's are defined so that $(a_j^{\dagger})^2 = 0$, which imposes the noncrossing condition. Hence the transfer matrix can be written as

$$\hat{T} = \hat{T}_0 \hat{T}_1 \hat{T}_2$$
$$= \exp\left[-\beta\eta_0 \sum_j a_j^{\dagger} a_j \right] \prod_i \left[1 + e^{-\beta\Gamma} (a_i^{\dagger} a_{i+1} + a_{i+1}^{\dagger} a_i) \right] \times \exp\left[-\beta \sum_{i<j} U_{ij} n_i n_j \right] ,$$

where $n_i = a_i^{\dagger} a_i$ and we have associated the interaction energy of the kth row with the $k \to k+1$ transfer matrix. We note in passing that $\hat{A}_i = a_i^{\dagger} a_{i+1} + a_{i+1}^{\dagger} a_i$ is idempotent, $\hat{A}_i^2 = \hat{A}_i$, and $\hat{A}_{i+1} \hat{A}_i = \hat{A}_i \hat{A}_{i+1}$. This allows $\hat{T}_1$ to be rewritten as

$$\hat{T}_1 \propto \prod_i e^{\beta J_1^* \hat{A}_i} ,$$

whence $\tanh\beta J_{\perp}^{*}=e^{-\beta\Gamma}$, yielding the dual transformation. Now let us take the continuum limit explicitly, following Fradkin and Susskind.[30] Let $\hat{T}=e^{-a_y\hat{H}}$ with $a_y\to 0$ and let $e^{-\beta\Gamma}$, η_0, and $U\to 0$ as a_y. Expanding both sides to order a_y we easily obtain

$$k_B T a_y \hat{H}=\eta_0\sum_i n_i+\sum U_{ij}n_i n_j-\frac{t}{2}\sum(a_i^{\dagger}a_{i+1}+a_{i+1}^{\dagger}a_i)\ ,$$

where $t=e^{-\beta\Gamma}/\beta$ is the hopping matrix element. This Hamiltonian is displayed in the main part of this paper in Eq. (3).

[1]C. Rottman and M. Wortis, Phys. Rev. B **29**, 328 (1984).

[2]C. Rottman and M. Wortis, Phys. Rep. **103**, 59 (1984). This paper reviews the field and gives many additional references.

[3]C. Jayaprakash, W. F. Saam, and S. Teitel, Phys. Rev. Lett. **50**, 2017 (1983).

[4]W. F. Saam, C. Jayaprakash, and S. Teitel, in *Quantum Fluids and Solids—1983,* edited by E. D. Adams and G. G. Ihas (AIP, New York, 1983), p. 371.

[5]A. F. Andreev, Zh. Eksp. Teor. Fiz. **80**, 2042 (1981) [Sov. Phys.—JETP **53**, 1063 (1982)].

[6]C. Rottman, M. Wortis, J. C. Heyraud, and J. J. Metois, Phys. Rev. Lett. **52**, 1009 (1984).

[7]F. Gallet, P. E. Wolf, and S. Balibar (unpublished).

[8]J. C. Heyraud and J. J. Metois, Acta Metal. **28**, 1789 (1980); J. Cryst. Growth **50**, 571 (1980).

[9]C. Jayaprakash and W. F. Saam, Phys. Rev. B **30**, 3916 (1984).

[10]The first reference for this model appears to be W. Kossel, Nachr. Ges. Wiss. Gottingen Math. Phys. Kl. 135 (1927). Gruber and Mullins (Ref. 11) refer to it as the terrace-ledge-kink model. We prefer step to ledge.

[11]E. E. Gruber and W. W. Mullins, J. Phys. Chem. Solids **28**, 875 (1967).

[12]V. L. Pokrovsky and A. L. Talapov, Phys. Rev. Lett. **42**, 65 (1979).

[13]J. Villain, in *Ordering in Strongly Fluctuating Condensed Matter Systems,* edited by T. Riste (Plenum, New York, 1980), p. 221.

[14]F. D. M. Haldane and J. Villain, J. Phys. (Paris) **42**, 1673 (1981).

[15]H. J. Schulz, B. I. Halperin, and C. L. Henley, Phys. Rev. B **26**, 3797 (1982). See also T. W. Burkhardt and P. Schlottmann, Z. Phys. B **54**, 151 (1984).

[16]See, e.g., G. Baym, *Lectures on Quantum Mechanics* (Benjamin, Reading, 1969), Chap. 19.

[17]V. I. Marchenko and A. Ya Parshin, Zh. Eksp. Teor. Fiz. **79**, 257 (1980) [Sov. Phys.—JETP **52**, 129 (1981)]. Here we refer to steps of the same sign.

[18]B. Sutherland, J. Math. Phys. **12**, 246 (1971); Phys. Rev. A **4**, 2019 (1971).

[19]See, e.g., E. Lieb, T. Schultz, and D. Mattis, Ann. Phys. (N.Y.) **16**, 407 (1961).

[20]C. N. Yang and C. P. Yang, (a) Phys. Rev. **150**, 321 (1966); (b) **150**, 327 (1966); (c) **151**, 258 (1966).

[21]See, e.g., J. des Cloizeaux, J. Math. Phys. **7**, 2136 (1966). This author considers only the half-filled-band case ($s=\frac{1}{2}$, $\eta=\eta_0+U$).

[22]This result is quite old and is due to L. D. Landau. See *Collected Papers of L. D. Landau,* edited by D. TerHaar (Pergamon, New York, 1965), p. 540.

[23]Y. He, C. Jayaprakash, and C. Rottman (unpublished).

[24]B. Krahl-Urban, E. A. Niekisch, and H. Wagner, Surf. Sci. **64**, 52 (1977). In this paper work-function data are used to extract dipole moments at steps on tungsten surfaces.

[25]M. D. Thompson and M. B. Huntington, Surf. Sci. **116**, 522 (1982).

[26]For example, xenon atoms adsorbed on Pd(100) have a dipole moment of $0.95D$. See P. W. Palmberg, Surf. Sci. **25**, 598 (1971).

[27]Dipolar, as well as elastic, effects occur in the commensurate-incommensurate transition problem as well. See Ref. 14.

[28]The enhancement is by a factor of 2 for dipoles oriented normal to a flat interface. See W. Kohn and K.-H. Lau, Solid State Commun. **18**, 553 (1976).

[29]V. I. Marchenko, Zh. Eksp. Teor. Fiz. **81**, 1141 (1981) [Sov. Phys.—JETP **54**, 605 (1982)].

[30]E. Fradkin and L. Susskind, Phys. Rev. D **17**, 2637 (1978).